ACS Catalysis

Article

Mechanistic Study on Deoxydehydration and Hydrogenation of Methyl Glycosides to Dideoxy Sugars over ReO-Pd/CeO catalyst

Ji Cao, Masazumi Tamura, Ryu Hosaka, Akira Nakayama, Jun-ya Hasegawa, Yoshinao Nakagawa, and Keiichi Tomishige

ACS Catal., **Just Accepted Manuscript** • DOI: 10.1021/acscatal.0c02309 • Publication Date (Web): 16 Sep 2020

Just Accepted

is published by the American Chemical Society. 1155 Sixteenth Street N.W., Washington, DC 20036

Mechanistic Study on Deoxydehydration and Hydrogenation of Methyl Glycosides to Dideoxy Sugars over ReO_x-Pd/CeO_2 Catalyst

Ji Cao[a], Masazumi Tamura*[b], Ryu Hosaka[c], Akira Nakayama[c, d], Jun-ya Hasegawa[c], Yoshinao Nakagawa[a] and Keiichi Tomishige*[a]

[a]Department of Applied Chemistry, School of Engineering, Tohoku University, 6-6-07, Aoba, Aramaki, Aoba-ku, Sendai 980-8579, Japan

[b]Research Center for Artificial Photosynthesis, Advanced Research Institute for Natural Science and Technology, Osaka City University, 558-8585, Japan

[c]Institute for Catalysis, Hokkaido University, Sapporo 001-0021, Japan

[d]Department of Chemical System Engineering, The University of Tokyo, Tokyo 113-8656, Japan

KEYWORDS Deoxydehydration, *Heterogeneous catalysis*, *Sugar conversion*, *Methyl glycoside*, *Rhenium*

ABSTRACT: We found that nonprotected methyl glycosides with *cis*-vicinal OH groups could be converted to the corresponding methyl dideoxy glycosides by deoxydehydration and consecutive hydrogenation (DODH+HG) over ReO_x-Pd/CeO_2 catalyst with gaseous H_2. In the study, the reactivity of the methyl glycosides in DODH was clearly lower than that of simple cyclic vicinal diols such as *cis*-1,2-cyclohexanediol and *cis*-1,2-cyclopentanediol, and the reactivity of the methyl glycosides was also different. Herein, we investigated the reactivity difference based on the kinetic studies and DFT calculations. The kinetic studies suggest that the reactivity difference between the methyl glycosides and the simple diols is derived from the OH group of methyl glycosides except the *cis*-vicinal diols, and that the reactivity difference among the methyl glycosides will be associated with the configuration of the substituents adjacent to the *cis*-vicinal diols, while the reaction mechanism of DODH is suggested to be basically similar judging from almost the same reaction orders with respect to substrate concentration and H_2 pressure in all substrates. The adsorption and transition states of methyl α-L-rhamnopyranoside and methyl α-L-fucopyranoside, which have large reactivity difference (methyl α-L-rhamnopyranoside >> methyl α-L-fucopyranoside), were estimated by DFT calculations with ReO_x/CeO_2 as the active site of ReO_x-Pd/CeO_2 catalyst, showing that the main difference is the activation energy in DODH of these substrates (65 kJ mol^{-1} for methyl α-L-rhamnopyranoside and 77 kJ mol^{-1} for methyl α-L-fucopyranoside), which was also supported by the results of the Arrhenius plots (63 kJ mol^{-1} and 73 kJ mol^{-1} for methyl α-L-rhamnopyranoside and methyl α-L-fucopyranoside, respectively). The activation energy was influenced by the torsional angle of the substituents adjacent to the *cis*-vicinal OH groups, which is derived from the interaction of the OH group adjacent to the *cis*-vicinal OH groups and the surface hydroxy groups on CeO_2.

INTRODUCTION

Biomass and their derivatives are oxygen-rich compared with fossil resources, and carbohydrates are one of the main components of biomass[1]. Selective reduction of the oxygen content is necessary to obtain valuable chemicals[2]. Some of the catalytic transformation of carbohydrates commonly lose their original stereostructure[3] despite that the stereostructure, particularly the chiral structures, was useful for the synthesis of valuable chemicals[4]. Some effective catalytic transformation methods of carbohydrate derivatives have been developed while maintaining their original stereostructure (Scheme 1). Muramatsu and co-workers found that an organotin catalyst provided high activity and regioselectivity for thiocarbonylation of nonprotected carbohydrates, and the obtained monothiocarbonates can be converted to the corresponding deoxy carbohydrates in good yields by Barton-McCombie reaction[5] (Scheme 1, A). Gagné and co-workers reported the pioneering work on the effective reaction system of $B(C_6F_5)_3$ + tertiary silane and $B(C_6F_5)_3$ + catecholborane for selective transformation of silyl-protected sugar alcohols to chiral polyol synthons[6] and reductive carbocyclization of silyl-protected unsaturated sugar alcohols to chiral cyclopentanes and cyclopropanes[7] (Scheme 1, B). Huber and co-workers demonstrated a novel transformation of cellulose to levoglucosenone[8], and furthermore substantiated transformation of levoglucosenone to chiral tetrahydrofurandimethanol and tetrahydropyran-2-methanol-5-ketone by hydrogenolysis[9] (Scheme 1, C). Toste and co-workers reported on the deoxydehydration (DODH) of various polyhydroxylated lactones using CH_3ReO_3 or $KReO_3$ with Pd/C catalyst to afford the corresponding chiral lactones in moderate yields (~88%)[10] (Scheme 1, D).

DODH reaction is a promising method to lower the oxygen content in carbohydrates and it can selectively transform vicinal OH groups to the corresponding C=C bond in a single step[11], and various homogeneous (such as Re[12]-, Ru[13]-,

Scheme 1. Examples of effective catalytic transformation methods of sugar derivatives to chiral products.

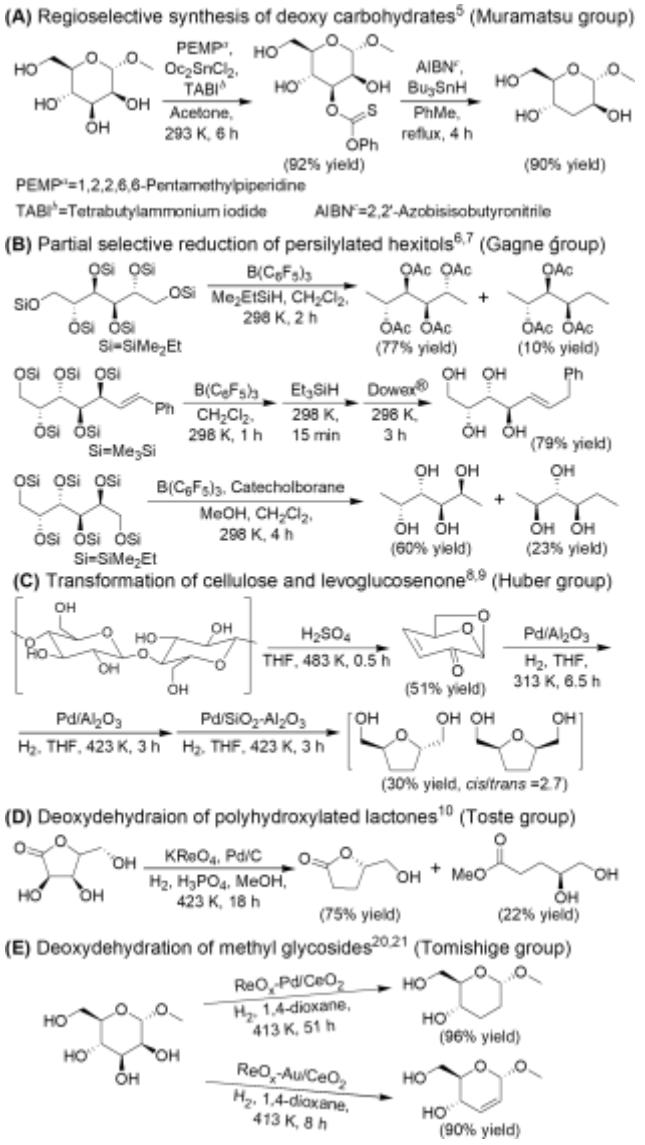

Mo[14]- and V[15]- based complexes) and heterogeneous (supported ReO_x[16] or MoO_x[17], bimetallic Pt-Re[18], ReO_x nanoparticles[19]) catalysts have been actively investigated. Recently, we firstly reported that Pd-modified CeO_2-supported Re (ReO_x-Pd/CeO_2)[20] and Au-modified CeO_2-supported Re (ReO_x-Au/CeO_2)[21] were effective and stable heterogeneous catalysts for the direct and selective transformation of the *cis*-vicinal OH groups in methyl glycosides without protection of OH groups by using gaseous H_2, providing the corresponding methyl dideoxy glycosides and methyl unsaturated dideoxy glycosides, respectively with retention of the original stereostructure (Scheme 1, E). The catalysts could be reused more than 4 times without loss of activity and selectivity with 125 turnover number (TON) based on the total Re atom of the catalyst[20]. These results are based on our previous finding of heterogeneous ReO_x-Pd/CeO_2 and ReO_x-Au/CeO_2 catalysts, which are effective for DODH + hydrogenation (HG) or DODH of polyols to alkanes[22] or alkenes[23], respectively, using gaseous H_2 as reductant. The turnover frequency (TOF) and TON per Re atom of ReO_x-Pd/CeO_2 (TOF: 300 h^{-1} at 443 K; TON: 10000 at 453 K for 96 h) were more than one order larger than those of previously reported catalysts[22]. The methyl saturated or unsaturated dideoxy glycosides are the core structure of natural products and important intermediates[24] for the synthesis of rare sugars, chiral ligands, medicines (*e.g.*, antibiotics, antitumor agents). In addition, the methyl dideoxy glycosides can be further converted to corresponding partially deoxy chiral acyclic polyols with high yield and high stereoselectivity[20,25], which can be used for the production of fine chemicals (*e.g.*, cosmetics, food additives, surfactants) and polymers (*e.g.*, alkyd resins, polyurethanes, polyesters).

According to our previous researches on DODH of simple diols over ReO_x-Pd/CeO_2 or ReO_x-Au/CeO_2 catalysts[20, 22b], the isolated Re^{4+} species on CeO_2 of these catalysts is catalytically active. The valence of the Re species was determined by XPS and XAS analyses, and the structure of the active site was proposed based on kinetic studies and/or DFT calculations in DODH + HG of 1,4-anhydroerythritol as a model diol[22b]. Pd or Au metals work as promoters for formation of the active Re^{4+} species via reduction of Re^{6+} species by H_2 activated by these metals. The CeO_2 support can suppress the over-reduction of Re species and stabilize the active isolated Re^{4+} species on the CeO_2 surface of the catalysts. The DODH reaction mechanism over the active Re^{4+} species formed on CeO_2 support was proposed to have three elementary reaction steps[22b] (Scheme 2): (i) Reduction of isolated Re^{6+} species to Re^{4+} species by activated H_2, (ii) coordination of the substrate with vicinal OH groups to the Re^{4+} species as diolate, and (iii) DODH of the diolate to form the corresponding alkenes and desorption of the produced alkene and regeneration of Re^{6+} center. In the case of DODH + HG of 1,4-anhydroerythritol[22b], the reaction orders with respect to the substrate concentrate and H_2 pressure were about zero, and the rate determining step is step (iii).

From the previous activity tests of methyl glycosides[20,22b], the reactivity is much lower than that of simple vicinal diols[22b], and the reactivity of methyl glycosides was changed by the type of methyl glycosides[20]. These results suggest that there will be some causes for the reactivity difference

Scheme 2. Proposed reaction mechanism of deoxydehydration (DODH) + hydrogenation (HG) over ReO_x–Pd/CeO_2 catalyst[22b].

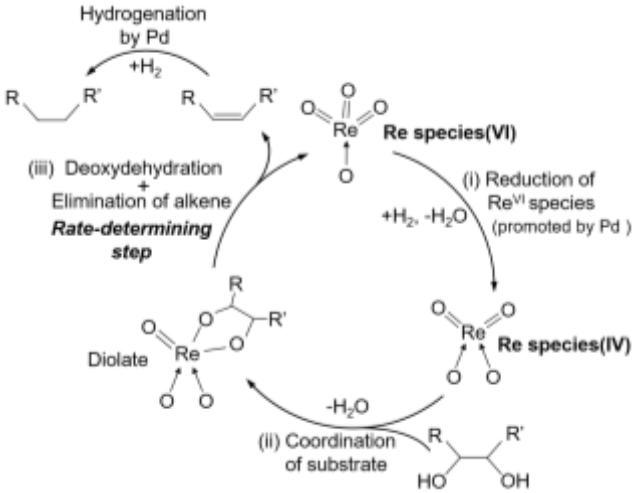

between the simple diols and methyl glycosides and that between the methyl glycosides. However, the causes are unclear, and compared with the simple diols, the methyl glycosides have other secondary OH groups, preliminary OH groups, and so on. In fact, to the best of our knowledge, there are no systematic research on the effect of the type and configuration of the substituents in pyranose- and furanose rings (such as OH, CH_2OH, OCH_3, CH_3 group and so on) except for *cis*-vicinal OH groups to the reactivity in DODH reaction. Therefore, clarification of the decisive factors to dominate the reactivity of the methyl glycosides is of great importance to elucidate the reaction mechanism of the DODH of methyl glycosides and the catalysis of ReO_x-based heterogeneous catalysts. We attempted to clarify the most important factor in the DODH reaction of methyl glycosides based on the systematic investigations, and it will provide useful information on the catalyst design for the transformation of sugar derivatives.

Herein, the kinetic parameters are determined in DODH + HG of methyl glycosides having *cis*-vicinal OH groups methyl α-D-mannopyranoside, methyl β-L-arabinopyranoside, methyl β-D-galactopyranoside and methyl α-L-(methyl β-D-ribofuranoside, methyl rhamnopyranoside, fucopyranoside) and related substrates (*cis*-1,2-cyclopentanediol, *cis*-1,2-cyclohexanediol and 1,4-anhydroerythritol) with ReO_x-Pd/CeO_2 catalyst. Moreover, the structures of the diolate intermediate and its transition state of methyl glycoside stereoisomers were calculated by DFT calculation with the catalytically active isolated Re species on CeO_2[22b]. The cause of the reactivity difference and the reaction mechanism of methyl glycosides were proposed based on the kinetics and DFT calculations.

RESULTS AND DISCUSSION

Screening of catalysts and reaction solvents in deoxydehydration (DODH) + hydrogenation (HG) of methyl α-D-mannopyranoside. At first, catalyst compositions, main DODH-active metal oxides, hydrogenation-active metals and supports, were investigated in DODH +HG of methyl α-D-mannopyranoside as a model reaction (Scheme 3, Figures S1-S5). The effect of the catalyst compositions was similar to that in the case of DODH+HG of 1,4-anhydroerythritol to tetrahydrofuran[22]: Re oxide is the most effective DODH-active metal oxide among various metal oxides ($M'O_x$; M'=V, Cr, Mn, Nb, Mo, W and Re) in terms of conversion and selectivity (Figure S1). Pd metal is an effective metal among various hydrogenation-active metals (M''=Co, Ni, Ru, Rh, Pd, Ag, Ir, Pt and Au) in terms of conversion and selectivity (Figure S2). CeO_2 was the most effective support among various metal oxides (MgO, γ-Al_2O_3, SiO_2, CaO, TiO_2, ZrO_2 and CeO_2) (Figure S3). Moreover, the optimized Re loading amount (2 wt%) (Figure S4) and Pd loading amount (Pd/Re ratio = 0.25) (Figure S5) of ReO_x-Pd/CeO_2 catalyst were also the

Scheme 3. DODH + HG of methyl α-D-mannopyranoside over ReO_x-Pd/CeO_2 catalyst.

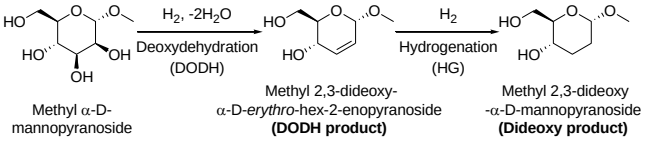

same as those in DODH+HG of 1,4-anhydroerythritol. ReO_x-Pd/CeO_2 (Re=2 wt%, Pd/Re=0.25) catalyst was used in the following studies.

Next, the solvent effect was investigated in the same reaction with ReO_x-Pd/CeO_2 (Figure S6). 1,4-Dioxane was the best solvent based on the activity and selectivity among various solvents, while some organic solvents with low polarity such as ethers (1,2-dimethoxyethane and tetrahydrofuran), alcohols (1-pentanol and 3-pentanol) and dodecane were good ones, showing similar conversion with high selectivity to the target dideoxy product in DODH + HG of methyl α-D-mannopyranoside. On the other hand, the conversion is a little low in the case of methanol, and water solvent provided almost no conversion. The low reactivity of methyl α-D-mannopyranoside in water solvent is also supported by the results of hydrolysis and hydrogenation of methyl dideoxy glycosides over supported Pt catalyst[25], where hydrolysis of methyl 3,4-dideoxy-glycosides is more difficult than that of methyl 2,3-dideoxy-glycoisdes in water solvent, which is probably because of the presence of OH group at C2 position[27]. One possible explanation of the result is the competitive adsorption of the solvents with the substrate. H_2O and methanol can be adsorbed on the catalyst surface by the OH group, and the adsorption of H_2O and methanol can suppress the adsorption of the substrates. Moreover, other reported DODH reaction systems[12d-g] also showed that the alcohol solvents would suppress the DODH reaction, which results are similar to that of this solvent effect.

The tendency is similar to the case of DODH+HG of 1,4-anhydroerythritol over ReO_x-Pd/CeO_2 catalyst in our previous work[22b].Considering that the solubility of sugar derivatives is typically low in organic solvents and high in water solvent, applicability of water-contained solvents is important. The mixed solvents of 1,4-dioxane and water were tested. In the case of 10 wt% water-contained 1,4-dioxane (1,4-dioxane : water = 9 : 1), the reaction hardly proceeded. When the water content decreased to 3 wt% (1,4-dioxane : water = 29 :1), the conversion (18%) was about half as low as that of only 1,4-dioxane (35%), and the selectivity to the product was a little low, which will be due to hydrolysis of the methyl α-D-mannopyranoside or its DODH product. Therefore, the catalyst tolerated a small amount of water, however, water is not a suitable solvent for the catalyst.

As above, the composition of ReO_x-Pd/CeO_2 (Re=2 wt%, Pd/Re=0.25) catalyst is the same as the case in DODH + HG of 1,4-anhydroerythritol[22], which implies that the active species and reaction mechanism of the DODH + HG are fundamentally similar. However, there are large reactivity difference between methyl glycosides and simple diols[22] as well as among various methyl glycosides[20]. Therefore, the further researches with methyl glycosides and related substrates based on the kinetic studies and DFT calculations are necessary to tease out the reasons.

Time-courses of methyl glycosides with *cis*-vicinal OH groups and the related substrates. Time-courses of DODH + HG of methyl glycosides with *cis*-vicinal OH groups (methyl β-D-ribofuranoside, methyl α-L-rhamnopyranoside, methyl α-D-mannopyranoside, methyl β-L-arabinopyranoside, methyl β-D-galactopyranoside and methyl α-cyclopentanediol and *cis*-1,2-cyclohexanediol) over ReO_x-Pd/CeO_2 (Re=2 wt%, Pd/Re=0.25) catalyst are shown in

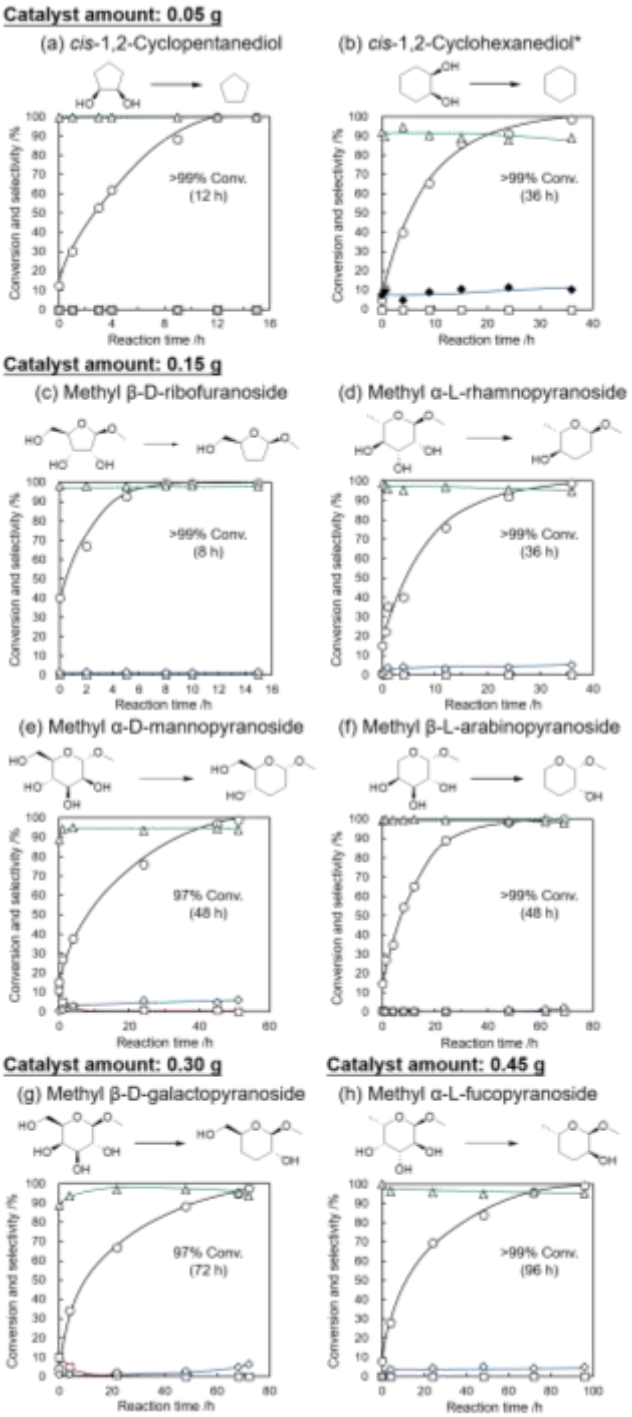

Figure 1. Time courses of DODH + HG of related substrates over ReO_x–Pd/CeO_2 (◯ and black lines: conversion; △ and green lines: selectivity to dideoxy product; □ and red lines: selectivity to DODH product; ◇ and blue lines: selectivity to other products, *◆: selectivity to *trans*-1,2-cyclohexanediol). Others contain methanol and degradation products. The detailed data are listed in Tables S1-S8. Reaction conditions: substrate 1.3 mmol, ReO_x–Pd/CeO_2 catalyst (0.05 g for *cis*-1,2-cyclopentanediol and *cis*-1,2-cyclohexanediol; 0.15 g for methyl β-D-ribofuranoside, methyl α-L-rhamnopyranoside, methyl α-D-mannopyranoside and methyl β-L-arabinopyranoside; 0.30 g for methyl β-D-galactopyranoside; 0.45 g for methyl α-L-fucopyranoside), 1,4-dioxane 10 g, 7.7 MPa H_2 at 413 K (initial 5.5 MPa H_2 at R.T.).

L-fucopyranoside) and simple cyclic vicinal diols (*cis*-1,2-Figure 1. The reaction time and catalyst amount were changed based on the reactivity of the substrates. All the substrates smoothly reacted to give high conversion (>99%). Taking the catalyst amount and reaction time for >99% conversion into consideration, the reactivity order of the substrates is as follows: *cis*-1,2-cyclopentanediol (a) > *cis*-1,2-cyclohexanediol (b) > methyl β-D-ribofuranoside (c) > methyl α-L-rhamnopyranoside (d) >methyl α-D-mannopyranoside (e) ≈ methyl β-L-arabinopyranoside (f) > methyl β-D-galactopyranoside (g) > methyl α-L-fucopyranoside (h).

The selectivity to the corresponding dideoxy product is totally high (>85%), however, the tendency of the selectivity is a little different among these substrates. The selectivity to the target product from *cis*-1,2-cyclopentanediol is very high (>99%, Figure 1(a), detailed data are in Table S1), however, the selectivity to cyclohexane from *cis*-1,2-cyclohexanediol is a little low even at low conversion level (10%, Figure 1(b), detailed data are in Table S2), and the main by-product is *trans*-1,2-cyclohexanediol. Generally speaking, the isomerization reaction of vicinal diols will proceed by dehydrogenation and subsequent hydrogenation. The stability of the five-membered ring ketones, *e.g.*, cyclopentanone, is lower than that of six-membered ring ketones, *e.g.*, cyclohexanone[28], which is due to the higher ring strain in the five-membered ring than that in the six-membered ring The selectivity difference between the reactions of *cis*-1,2-cyclopentanediol and *cis*-1,2-cyclohexanediol could be explained by the stability of their ketone intermediates. The dehydrogenation of *cis*-1,2-cylcopentanediol may be more difficult to occur than that of 1,2-cyclohexanediol on ReO_x-Pd/CeO_2 catalyst due to the lower stability of the intermediate of 2-hydroxycyclopentanone than 2-hydrxycyclohexanone[28].

Isomerized product was not detected in the cases of methyl glycosides including ones with a six-membered ring, which result is different behavior from that of 1,2-cyclohexanediol. In order to compare the difference of selectivity to isomerization product between simple cyclic diols and methyl glycosides, four six-membered ring substrates (*trans*-1,2-cyclohexanediol, *cis*-1,2-cyclohexanediol, methyl α-D-mannopyranoside, methyl α-D-glucopyranoside) are picked up, and their energy changes (ΔE) in dehydrogenation or isomerization are estimated by DFT calculation (Table S9). The results showed that ΔE from dehydrogenated intermediate to the corresponding isomers with respect to the substrate is different: the ΔE of cyclic diols from 2-hydroxycyclohexanone + H_2 (74.1 kJ mol^{-1} for *trans*-1,2-cyclohexanediol, and 71.9 kJ mol^{-1} for *cis*-1,2-cyclohexanediol) is clearly smaller than the ΔE of methyl glycosides from 2-dehydrogenated methyl α-D-glucopyranoside + H_2 (99.2 kJ mol^{-1} for methyl α-D-glucopyranoside, and 86.5 kJ mol^{-1} for methyl α-D-mannopyranoside), suggesting the lower barrier for dehydrogenation of 1,2-cyclohexanediols. In addition, in the case of methyl glycosides as substrates, the ΔE of methyl α-D-mannopyranoside (86.5 kJ mol^{-1}) is quite lower than that of methyl α-D-glucopyranoside (99.2 kJ mol^{-1}), Therefore, it can be concluded that the epimerization is more difficult to occur in methyl glycosides than the simple 1,2-cyclohexanediols.

As for the selectivity, methyl β-D-ribofuranoside (Figure 1(c), detailed data are in Table S3) having a five-membered ring showed high selectivity to the dideoxy product with a little byproduct, such as 1-pentanol and tetrahydrofurfuryl alcohol (THFA). On the other hand, in the case of methyl glycosides having a six-membered ring, the selectivity depends on the type of methyl glycosides. Methyl β-L-arabinopyranoside showed high selectivity at any reaction time, and high yield of the target dideoxy product (99% at 62 h) was obtained (Figure 1(f), detailed data are in Table S6). Methyl α-D-mannopyranoside and methyl β-D-galactopyranoside, which are stereoisomers (Figures 1(e) and (g), detailed data are in Table S5 and S7), provided the DODH product as an intermediate (selectivity is 5~11%) below 30% conversion level. However, since the DODH product is an intermediate of the dideoxy product, the selectivity to the dideoxy product can increase with increasing the conversion level. Methyl α-L-rhamnopyranoside and methyl α-L-fucopyranoside, which are also stereoisomers, showed high selectivity to the dideoxy product at low conversion level and the selectivity gradually decreased by the side reactions such as hydrolysis and/or hydrogenolysis of C-O bonds (Figures 1(d) and (h), detailed data are in Tables S4 and S8). Among all the methyl glycosides having a six-membered ring, methyl α-D-mannopyranoside and methyl β-D-galactopyranoside showed higher selectivity to DODH product at low conversion level than the other methyl glycosides, which can be interpreted by the lower hydrogenation ability of these two kinds of DODH products. Furthermore, the selectivity to DODH products decreased with reaction time, suggesting that the hydrogenation ability also depended on the concentration of the DODH products.

As above, the selectivity to the target product is totally high, except at the very high conversion level for some methyl glycosides having a six-membered ring, which means that the side reactions will be much slower than the DODH reaction, and the difference of the substituents except *cis*-vicinal OH groups and the configuration will not influence the selectivity so strongly. On the other hand, the reactivity of methyl glycosides is pretty different, and the substituents except *cis*-vicinal OH groups and the configuration may influence the adsorption state and transition state.

Kinetic studies on DODH + HG of various methyl glycosides and the related diols over ReO_x-Pd/CeO_2 catalyst. To clarify the difference of the reactivity among the methyl glycosides and the related diols, precise investigation of the effect of kinetic parameters is essential. During the kinetic reaction, ReO_x-Pd/CeO_2 catalyst (more than 50 g) was prepared in one batch and used in order to eliminate the preparation errors of the catalysts. To measure the reaction rate more precisely, the initial H_2 pressure in autoclave was decreased from 5.5 MPa to 1.0 MPa at R.T. in the kinetic studies to decrease the conversion at 0 h (< 15%), and the reaction rate was estimated from the slope of the three points at different reaction times at low conversion level below 35% based on the formation amount of DODH product + dideoxy product. The reaction rate (mmol g_{cat}^{-1} h^{-1}) was estimated by the following equation: Reaction rate (mmol g_{cat}^{-1} h^{-1}) = (slope [mmol/h]/ (catalyst amount [g_{cat}]). The experimental error of the reaction rates was estimated by three times reactions with methyl α-D-mannopyranoside as a model substrate under the standard reaction conditions, and the error range of the reaction rate was estimated to be about 3% (1.7±0.04 (Figure S7)).

Simple cyclic vicinal diols (*cis*-1,2-cyclopentanediol, 1,4-anhydroerythritol and *cis*-1,2-cyclohexanediol) and methyl glycosides (methyl β-D-ribofuranoside, methyl α-L-rhamnopyranoside, methyl α-D-mannopyranoside, methyl β-L-arabinopyranoside, methyl β-D-galactopyranoside and methyl α-L-fucopyranoside) were used as substrates for

Table 1. Reaction rates and reaction orders of the methyl glycosides and the related substrates over ReO_x-Pd/CeO_2 catalyst

Entry	Substrate	Reaction rate[a] /mmol g_{cat}^{-1} h^{-1}	Reaction order	
			Concentration[b]	H_2 Pressure[c]
1*	 *cis*-1,2-Cyclopentanediol	20	-0.1	0.2
2*	 1,4-Anhydroerythritol	9.0	-0.3	0.1
3*	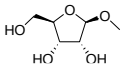 Methyl β-D-ribofuranoside	4.5	0.1	0.1
4	 *cis*-1,2-Cyclohexanediol	7.2	0.0	0.1
5	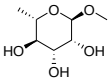 Methyl α-L-rhamnopyranoside	1.9	0.1	0.2
6	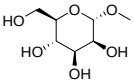 Methyl α-D-mannopyranoside	1.7	-0.1	0.3
7	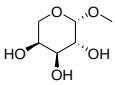 Methyl β-L-arabinopyranoside	1.7	0.0	0.2
8	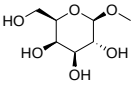 Methyl β-D-galactopyranoside	0.73	-0.1	0.2
9	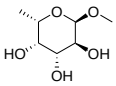 Methyl α-L-fucopyranoside	0.38	0.0	0.3

Reaction conditions: ReO_x-Pd/CeO_2 catalyst 0. 15 g (Re=2 wt%, Pd/Re=0.25), substrate amount 1.3 mmol (*substrate amount 3.9 mmol), 1,4-dioxane 10 g, 7.7 MPa H_2 at 413 K (initial 1.0 MPa H_2 at R.T.), 413 K. [a]The detailed reaction rate data are shown in Figure S8, [b]the detailed data are shown in Figures S9 and S10, [c]the detailed data are shown in Figures S11 and S12.

measurement of the reaction rate, and the results shown are separated into substrates with a five-membered ring (entries 1-3) and substrates with a six-membered ring (entries 4-9) in Table 1 (detailed data are listed in Figure S8). The order of the reaction rates is as follows: *cis*-1,2-cyclopentanediol > 1,4-anhydroerythritol > *cis*-1,2-cyclohexanediol > methyl β-D-ribofuranoside > methyl α-L-rhamnopyranoside > methyl α-D-mannopyranoside ≈ methyl β-L-arabinopyranoside > methyl β-D-galactopyranoside > methyl α-L-fucopyranoside. This order agrees well with that of the time-courses results in Figure 1. The simple cyclic vicinal diols gave higher reaction rate (7.2~20 mmol g_{cat}^{-1} h^{-1}, entries 1, 2 and 4) than the methyl glycosides (0.38~4.5 mmol g_{cat}^{-1} h^{-1}, entries 3 and 5-9). As for the substrates with a five-membered ring, the reaction rate of 1,4-anhydroerythritol having a tetrahydrofuran ring (9.0 mmol g_{cat}^{-1} h^{-1}, entry 2) is about 1/2-fold lower than that of *cis*-1,2-cyclopentanediol (entry 1), which will be related to the presence of the O atom in the ring. On the other hand, methyl β-D-ribofuranoside having a tetrahydrofuran ring showed the reaction rate of 4.5 mmol g_{cat}^{-1} h^{-1} (entry 3), which is about 1/2-fold than that of 1,4-anhydroerythritol (9.0 mmol g_{cat}^{-1} h^{-1}, entry 2). Considering the structure difference between methyl β-D-ribofuranoside and 1,4-anhydroerythritol (entries 2 and 3), the decrease of the reactivity will be derived from the methoxy group at C1 position and/or hydroxymethyl group at C4 position of the tetrahydrofuran ring in methyl β-D-ribofuranoside.

Regarding the substrates with a six-membered ring, *cis*-1,2-cyclohexanediol (entry 4) showed higher reaction rate than methyl glycosides (entries 5-9), which tendency is similar to that of substrates with a five-membered ring. The decrease of the reactivity may be explained by the presence of the O atom in the ring and the other substituents except *cis*-vicinal OH groups. Among the methyl glycosides having a six-membered ring (entries 4-9), there are reactive methyl glycosides (methyl α-L-rhamnopyranoside, methyl α-D-mannopyranoside and methyl β-L-arabinopyranoside, entries 5-7) and less-reactive methyl glycosides (methyl β-D-galactopyranoside and methyl α-L-fucopyranoside, entries 8 and 9). The reactive methyl glycosides showed the reaction rate of 1.7-1.9 mmol g_{cat}^{-1} h^{-1} (entries 5-7), and the less-reactive methyl glycosides showed lower reaction rate (0.73 and 0.38 mmol g_{cat}^{-1} h^{-1}, entries 8 and 9). We focus on the functional groups and the configuration of the substituents adjacent to the *cis*-vicinal OH groups in the substrates. The adjacent functional groups in the reactive methyl glycosides (entries 5-7) tend to be at the opposite side to the *cis*-vicinal OH groups, not at the same side. In contrast, one of the adjacent functional groups in the less-reactive methyl glycosides (entries 8 and 9) tends to be at the same side to the *cis*-vicinal OH groups: CH_2OH group (methyl β-D-galactopyranoside, entry 8) and CH_3 group (methyl α-L-fucopyranoside, entry 9) at C6 position. These results suggest that the adjacent functional group at the same side to the *cis*-vicinal OH groups will decrease the reactivity of the DODH reaction. In addition, methyl β-L-arabinopyranoside and methyl α-D-mannopyranoside showed similar reaction rates (1.7 mmol g_{cat}^{-1} h^{-1}, entries 6 and 7), although methyl α-D-mannopyranoside has a CH_2OH group at the C6 position, the β-position of the *cis*-vicinal OH groups. The CH_2OH group in the methyl α-D-mannopyranoside is located on the opposite side of the *cis*-vicinal OH groups. Therefore, the similar reactivity of methyl α-D-mannopyranoside and methyl β-L-arabinopyranoside can be interpreted by almost no interaction of the CH_2OH group in methyl α-D-mannopyranoside with the Re diolate.

Finally, the reactivity difference between the substates with a five-membered ring and those with a six-membered ring was compared. In the case of simple cyclic diols, the reaction rate of *cis*-1,2-cyclopentanediol (20 mmol g_{cat}^{-1} h^{-1}, entry 1) is 3-fold higher than that of *cis*-1,2-cyclohexanediol (7.2 mmol g_{cat}^{-1} h^{-1}, entry 4). This reaction rate difference is similar to that between the reactive methyl glycosides (1.7-1.9 mmol g_{cat}^{-1} h^{-1}, entries 5-7) and methyl β-D-ribofuranoside having a five-membered ring (4.5 mmol g_{cat}^{-1} h^{-1}, entry 3) (about 3-fold). Therefore, the reactivity of the substrates with a five-membered ring will be higher than that of the substrates with a six-membered ring, and the reactivity difference can be reflected by the difference of the ring structure, a six-membered ring or five-membered one.

According to our previous works on hydrogenolysis of glycerol and erythritol over metal oxide-modified noble metal catalysts[29], primary OH groups can be more easily adsorbed on the metal oxide species than secondary OH groups. The adsorption property of OH groups may influence the reactivity of methyl glycosides. The results of methyl α-L-rhamnopyranoside (entry 5) and methyl α-D-mannopyranoside (entry 6), which have the same functional groups except for the functional group at the C6 position (CH_3 group in methyl α-L-rhamnopyranoside (entry 5), CH_2OH group in methyl α-D-mannopyranoside (entry 6)) showed that the reactivities are similar, suggesting that the effect of the primary OH group in the CH_2OH group is not so large. Moreover, the reaction of 1,4-anhydroerytheritol in the presence of tetrahydrofurfuryl alcohol as a model alcohol having a primary OH group was performed with

Scheme 4. Effect of addition of primary alcohol in the DODH + HG of 1,4-anhydroerythritol over ReO_x-Pd/CeO_2 catalyst

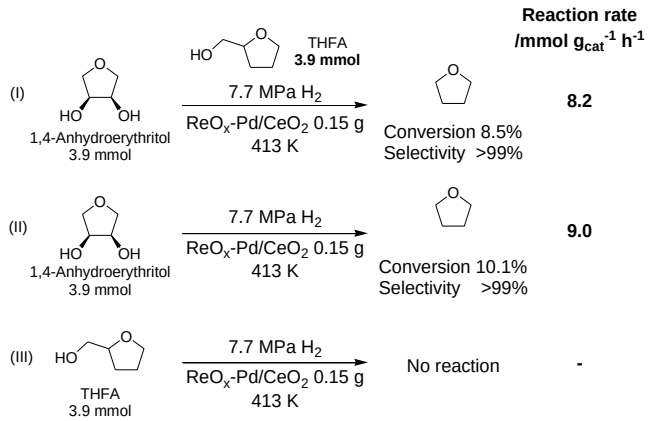

(I): The DODH + HG of 1,4-anhydroerythritol over ReO_x-Pd/CeO_2 catalyst in the presence of THFA; (II): the DODH + HG of 1,4-anhydroerythritol over ReO_x-Pd/CeO_2 catalyst; (III): the DODH + HG of THFA over ReO_x-Pd/CeO_2 catalyst. The detailed reaction rate data are shown in Table S11. Reaction conditions: ReO_x-Pd/CeO_2 catalyst 0. 15 g (Re=2 wt%, Pd/Re=0.25), 3.9 mmol for each substrate, 1,4-dioxane 10 g, 7.7 MPa H_2 at 413 K (initial 1.0 MPa H_2 at R.T.), 413 K.

Scheme 5. Effect of addition of dideoxy product in the DODH + HG of methyl α-D-mannopyranoside over ReO_x-Pd/CeO_2 catalyst

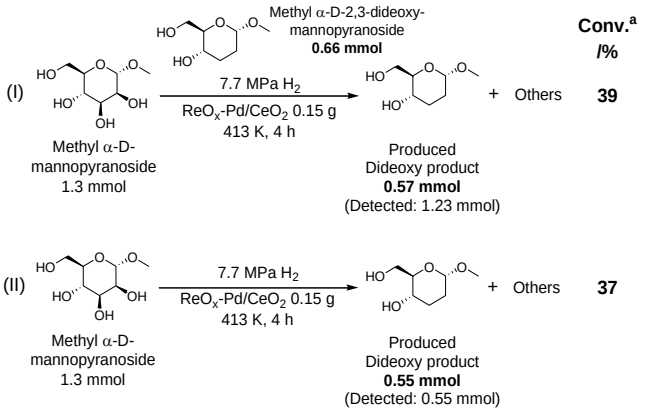

(I): The DODH + HG of methyl α-D-mannopyranoside over ReO_x-Pd/CeO_2 catalyst in the presence of dideoxy product; (II): the DODH + HG of methyl α-D-mannopyranoside over ReO_x-Pd/CeO_2 catalyst. The detailed data are shown in Table S12. Reaction conditions: ReO_x-Pd/CeO_2 catalyst 0. 15 g (Re=2 wt%, Pd/Re=0.25), methyl α-D-mannopyranoside 1.3 mmol, additive dideoxy product amount 0.6 mmol, 1,4-dioxane 10 g, 7.7 MPa H_2 at 413 K (initial 1.0 MPa H_2 at R.T.), 4 h, 413 K. [a]Calculated on inputted methyl α-D-mannopyranoside basis.

ReO_x-Pd/CeO_2 catalyst (Scheme 4(I), the detailed data are shown in Table S11). The reaction rate of 1,4-anhydroerytheritol was not so changed in the absence/presence of THFA (Scheme 4(I) and (II)). Certainly, it was confirmed that THFA did not react at all over ReO_x-Pd/CeO_2 catalyst (Scheme 4(III)). Therefore, primary OH group did not suppress the adsorption of the *cis*-vicinal OH groups, probably suggesting that the adsorption strength of the *cis*-vicinal OH groups is stronger than that of primary OH groups. This result also supported the similar reaction rates of methyl β-L-arabinopyranoside and methyl α-D-mannopyranoside (1.7 mmol g_{cat}^{-1} h^{-1}, entries 6 and 7, Table 1) despite the presence of CH_2OH group at the C6 position in methyl α-D-mannopyranoside.

There is a possibility that the produced dideoxy product influences the reactivity of methyl glycosides. In order to check the effect of the dideoxy product on the DODH reaction rate, the activity test of methyl α-D-mannopyranoside was carried out in the presence of the corresponding dideoxy product, methyl α-D-2,3-dideoxy mannopyranoside (Scheme 5(I), the detailed data are shown in Table S12). The conversion was similar to that of only methyl α-D-mannopyranoside (Scheme 5(II)). Therefore, the dideoxy product did not affect the reaction. Considering that the dideoxy product has 1,3-diol structure at C4 and C6 which can be adsorbed on the active site of Re^{4+} species, the adsorption strength of the *cis*-vicinal OH groups in the methyl glycosides on the active site will be larger than that of 1,3-diol.

Next, the reaction orders with respect to the substrate concentration and H_2 pressure were investigated with all the model substrates. The results are also listed in Table 1, and the details are shown in Figure S8-S11. The experimental error of the reaction order was estimated based on the error range of the reaction rate (~3%), and the reaction order of methyl α-D-mannopyranoside as a model substrate was estimated to be -0.1±0.03 (Figure S7 (b)). The reaction orders with respect to the substrate concentration were estimated to be almost zero in all the substrates, which suggests that the coverage of the substrates on the active site is almost saturated under the reaction conditions because of the strong adsorption of methyl glycosides at *cis*-vicinal OH groups, and the rate-determining step is not the coordination of the substrate with the *cis*-vicinal OH groups to the Re^{4+} species as diolate (step (ii), Scheme 2). The reaction orders with respect to the H_2 pressure were estimated to be also almost zero in all the substrates, suggesting that the reaction related with hydrogen is not included in the rate-determining step. The result excludes the possibility that the rate-determining step is the step (i) in Scheme 2. These results agree with those of the previous works on the DODH + HG mechanism of 1,4-anhydroerythritol over ReO_x-Pd/CeO_2 catalyst[22b], demonstrating that the reaction mechanism of methyl glycosides is similar to the proposed one, and the rate-determining step is the DODH reaction and the elimination of alkene from the diolate adspecies on ReO_x-Pd/CeO_2 catalyst.

In order to clarify the reactivity difference among the methyl glycosides having a six-membered ring, we selected methyl α-L-rhamnopyranoside and methyl α-L-fucopyranoside as model substrates because these substrates are stereoisomers and the reactivity difference is very large (about 5-fold; methyl α-L-rhamnopyranoside: 1.9 mmol g_{cat}^{-1} h^{-1}, methyl α-L-fucopyranoside: 0.38 mmol g_{cat}^{-1} h^{-1}, Table 1, entry 5 and 9). The effect of the reaction temperature was

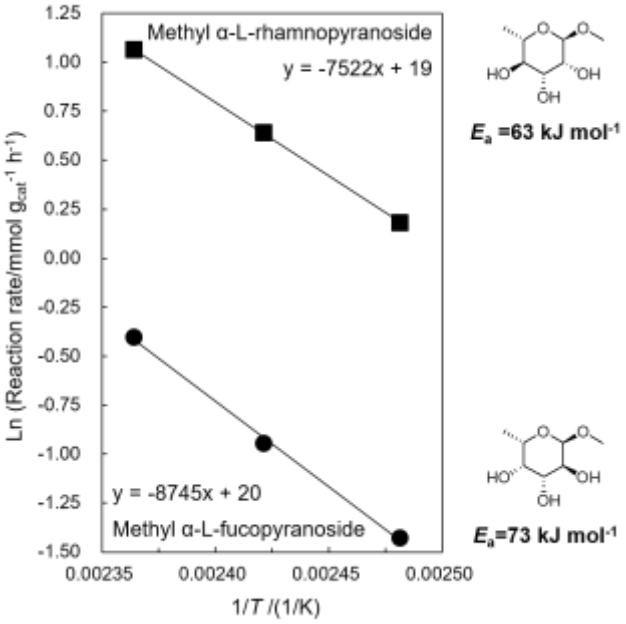

Figure 2. Arrhenius plots of DODH + HG of methyl α-L-rhamnopyranoside (■) and methyl α-L-fucopyranoside (●) over ReO_x-Pd/CeO_2 catalyst. Reaction conditions: ReO_x-Pd/CeO_2 catalyst 0.15 g (Re=2 wt%, Pd/Re=0.25), substrate 1.3 mmol, 1,4-

dioxane 10 g, 7.7 MPa H_2 (initial 1.0 MPa H_2 at R.T.), 403-423 K. The detailed data are shown in Table S13.

investigated with these methyl glycosides. Arrhenius plots of these substrates provided linear lines (Figure 2, the detailed data are shown in Table S13). The Arrhenius plots provided similar Y intercepts of these substrates (19±1 for methyl α-L-rhamnopyranoside and 20±1 for methyl α-L-fucopyranoside). The apparent activation energies of methyl α-L-rhamnopyranoside and methyl α-L-fucopyranoside are estimated to be 63±4 and 73±4 kJ mol^{-1}, respectively. Considering that the reaction mechanism of these methyl glycosides is similar based on the kinetic studies as discussed above (Table 1), the reactivity difference between these methyl glycosides can be attributed to the difference of the apparent activation energies. These results suggest that the transition states or adsorption states in the DODH of methyl α-L-rhamnopyranoside and methyl α-L-fucopyranoside are different, which can be derived from the difference of substituents and their configuration adjacent to the *cis*-vicinal OH groups in these methyl glycosides.

DFT calculation of DODH reaction of methyl α-L-rhamnopyranoside and methyl α-L-fucopyranoside over ReO_x-Pd/CeO_2 catalyst. The adsorption state of the selected methyl glycosides (methyl α-L-rhamnopyranoside and methyl α-L-fucopyranoside, labeled as **1** and **2**, respectively) was estimated by DFT calculation with the isolated Re^{4+} species on CeO_2, which is the active site of ReO_x-Pd/CeO_2 catalyst[22b], and moreover, the transition state in DODH reaction of these two methyl glycosides was also determined. The periodic-boundary DFT with plane-wave basis set was employed in this investigation using the VASP pack-age (computational details are given in Experimental in SI).

Since the CeO_2 surface is exposed to high H_2 pressure, fully hydrogenated surface is considered in this investigation. To accommodate the monomeric ReO_x species on the surface, three hydrogen atoms are removed from the surface and ReO_x species is placed on it to bind to three surface O atoms. When comparing the stability of various ReO_x species with the different number of oxygen atoms (x = 0 ~ 2), we found that the ReO_x (x = 1) species on three O atom of CeO_2 is the most stable structure over the surface (see the computational details in SI), which is in accordance with the recent work[30]. In this structure, which we refer to model-I hereafter (Figure S13), the oxidation state of Re atom is estimated as +7 based on the number of reduced Ce^{3+} atoms in the system. This oxidation state is different from the experimental observations, where the active Re species involves the oxidation state of +4. Because of this, we also consider the model where one of the three bridging O atoms is removed from model-I. In this model, which is referred as model-II (Figure S13), the Re atom is bound to two surface O atoms, and the oxidation state of Re is calculated to be +4, which is in accordance with the experimental findings (see Figure S13 for both structures). Using these two active site models, we compare the stability of intermediate diolate adspecies of the substrate. In the case of substrate **1**, we found that the adsorption energy (E_{ad}) of the most stable diolate adspecies over model-II is −32 kJ mol^{-1}, while it is 126 kJ mol^{-1} for model-I (structures are given in Figure S13). Therefore, the model-II would be the most plausible structure of active species of the ReO_x/CeO_2 catalyst.

According to our previous reports on DODH + HG of methyl glycosides[20], only the *cis*-vicinal OH groups in methyl glycosides can be selectively removed, however, *trans*-vicinal OH groups in methyl glycosides can be adsorbed on the active sites of ReO_x-Pd/CeO_2 catalyst as a diolate, which may suppress the reaction. Therefore, we calculated the adsorption energies of the selected stereoisomers (**1** or **2**) at *cis*-vicinal OH groups and *trans*-vicinal OH groups. There are two conformations for each diolate structure (*cis*-vicinal OH groups and *trans*-vicinal OH groups) depending on the orientation. Four kinds of diolate adspecies were determined for the two methyl glycosides, and denoted as *cis*-A, *cis*-B, *trans*-A, *trans*-B (*cis*-A**1**, *cis*-B**1**, *trans*-A**1**, *trans*-B**1** in Figure S14, and *cis*-A**2**, *cis*-B**2**, *trans*-A**2**, *trans*-B**2** in Figure S15). Among these diolate adspecies, *cis*-A adsorption conformation showed the lowest E_{ad} (-32 kJ mol^{-1} for *cis*-A**1** and –30 kJ mol^{-1} for *cis*-A**2**), indicating that the adsorption of *cis*-vicinal OH group is stronger than that of *trans*-OH group on ReO_x species. Hereafter, we only focus on the most stable conformation, *cis*-A.

Figure 3(a) shows the structure of diolate adspecies of **1**, and it is reclined to the surface involving the hydrogen bond with the surface hydroxy groups. The transition state structure for the cleavage of two C-O bonds is given in Figure 3 (b), and it exhibits asymmetric structure with respect to the dissociation of the two C-O bonds, and one bond length is 1.71 Å and the other is 2.01 Å. This could be mainly due to the stabilization of O2 (shown in the figure) which fills the vacancy site after releasing the DODH product, in addition to the hydrogen bond with the surface. The activation energy $E_{barrier\text{-}1}$ is calculated to be 65 kJ mol^{-1}, which is in good agreement with the experimental value of $E_{a\text{-}1}$ = 63 kJ mol^{-1}.

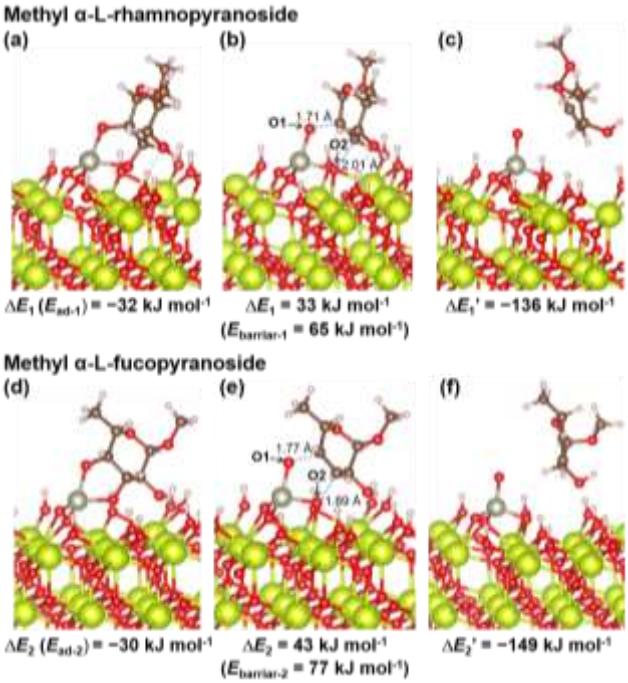

Figure 3. Structures of (a) diolate, (b) transition state and (c) the final product of **1**, and (d) diolate, (e) transition state and (f) the final product of **2**. White, dark brown, red, gray

and green balls represent hydrogen, carbon, oxygen, rhenium and cerium atoms, respectively.

After releasing the DODH product, the ReO species is bound to three surface O atoms (Figure 3(c)).

Figure 3 (d-f) shows the structures of diolate adspecies, transition state, and the final product for methyl α-L-fucopyranoside. The structures of ReO/CeO_2 catalyst are similar to those of **1**. The E_{ad} of diolate adspecies is very close, −32 kJ mol^{-1} for $E_{ad\text{-}1}$ and −30 kJ mol^{-1} for $E_{ad\text{-}2}$. A closer look into the transition structure of **2** shows that asymmetry with respect to the cleavage of the two C-O bonds is less pronounced, and the O2 atom is less stabilized in comparison to **1**. The calculated activation energy $E_{barriar\text{-}2}$ of 77 kJ mol^{-1} is slightly higher than that of $E_{barriar\text{-}1}$, which is also in good agreement with the experimental value of $E_{a\text{-}2}$ = 73 kJ mol^{-1}.

As a model calculation, the gas-phase DODH reaction of methyl glycosides with CH_3ReO_3 catalyst is investigated by using the Gaussian 09 package (Figure S16, and computational details are given in Experimental in SI). The DFT calculation for mechanism of the homogeneous CH_3ReO_3-catalyzed DODH of glycols was carried out by Nicolas and Liu[31], and the calculated structure around the Re center in the transition state was similar to those by our calculation. The activation energies of **1** and **2** are calculated as $\Delta E_{TS\text{-}1}$ = 87 kJ mol^{-1} and $\Delta E_{TS\text{-}2}$ = 83 kJ mol^{-1}, respectively, indicating that the activation energies of these substrates on CH_3ReO_3 are very close to each other. The difference in the structures at the transition state over the active sites of ReO/CeO_2 comes from the intricate interactions between the adjacent functional groups to *cis*-vicinal OH groups and the surface hydroxy groups.

Focusing on the structures of these methyl glycosides in

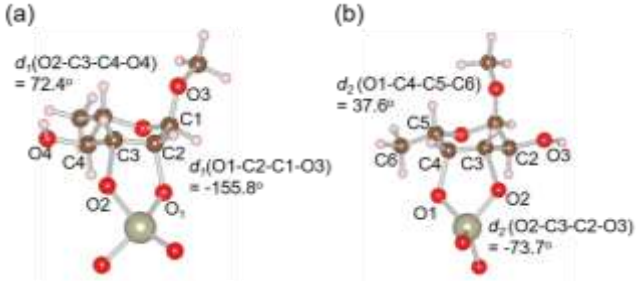

Figure 4. Extracted structures of the transition states of (a) **1** and (b) **2** over ReO_x/CeO_2 in Figure 3. White, dark brown, red, gray and green balls represent hydrogen, carbon, oxygen, rhenium and cerium atoms, respectively.

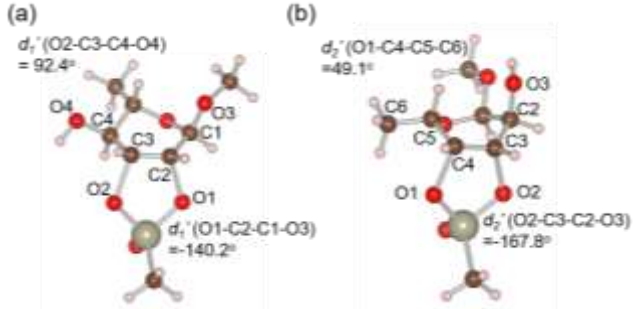

Figure 5. Extracted structures of the transition states of (a) **1** and (b) **2** on CH_3ReO_3 in Figure S16. White, dark brown, red, gray and green balls represent hydrogen, carbon, oxygen, rhenium and cerium atoms, respectively.

the transition state, the configuration and torsional angle are clearly different. The extracted transition structure and torsional angle on CH_3ReO_3 and ReO_x/CeO_2 are shown in Figures 4 and 5. The configuration of **1** and **2** over ReO_x/CeO_2 (Figure 4) was chair one. The torsional angle (*d*) with respect to the C-O bonds of the diolate is different: the d_1(O2-C3-C4-O4) of **1** (72.4°) is similar to the d_2(O2-C3-C2-O3) of **2** (-73.7°), however the d_1(O1-C2-C1-O3) of **1** (-155.8°) is quite different from the d_2(O1-C4-C5-C6) of **2** (37.6°), and the difference is very large. In general, low torsional angle decreases the stability of the structure, meaning the de crease of stability of the transition state. Therefore, it can be concluded that the difference of the activation energy between **1** and **2** is derived from the stability difference of the transition states induced by the difference of the torsional angles, one of the steric effects.

On the other hand, in the case of CH_3ReO_3 (Figure 5), the configuration of **1** was chair one, however, that of **2** was boat one, which is different from that in the case of ReO_x/CeO_2. As for the torsional angle, **1** provided d_1'(O2-C3-C4-O4) of 92.4° and d_1'(O1-C2-C1-O3) of -140.2°, which are similar to those in the case of ReO_x/CeO_2 (d_1(O2-C3-C4-O4)= 72.4°, d_1(O1-C2-C1-O3)= -155.8°). In contrast, **2** gave d_2'(O1-C4-C5-C6) of 49.1° and d_2'(O2-C3-C2-O3) of -167.8°, which are different from those in the case of ReO_x/CeO_2(d_2(O1-C4-C5-C6)= 37.6°, d_2(O2-C3-C2-O3)= -73.7 °). The large torsional angle of d_2'(O2-C3-C2-O3) (-167.8°) was formed by the conformation change from the boat to chair one, which can release the steric effect. This result was supported by the similar activation energies on CH_3ReO_3 catalyst (Figure S16). Therefore, the difference of activation energy over ReO_x/CeO_2 between **1** and **2** can be also explained by the result that the boat conformation was not formed on ReO_x/CeO_2, and the confinement is due to the interaction of the OH group (O3) with the OH groups on CeO_2 surface (Figure 3).

Based on the above results, the conformation of the adspecies of methyl glycosides on ReO_x/CeO_2 was confined by the interaction between the functional groups in methyl glycosides and the surface OH groups, and in the case of methyl α-L-fucopyranoside, the conformation confinement resulted in the low torsional angle, which will lead to high activation energy.

CONCLUSIONS

The screening of the active metal oxides, noble metals, supports and solvents in the DODH+HG of methyl glycosides showed that the same catalyst of ReO_x-Pd/CeO_2 (Re=2 wt%, Pd/Re=0.25) was effective for the reaction as in the case of DODH+HG of 1,4-anhydroerythritol.

Kinetic studies were performed with the ReO_x-Pd/CeO_2 catalyst by using various methyl glycosides with *cis*-vicinal OH groups (methyl β-D-ribofuranoside, methyl α-L-rhamnopyranoside, methyl α-D-mannopyranoside, methyl β-L-arabinopyranoside, methyl β-D-galactopyranoside and methyl α-L-fucopyranoside) and the related cyclic vicinal diols (*cis*-1,2-cyclopentanediol, 1,4-anhydroerythritol and *cis*-1,2-cyclohexanediol). The substituents adjacent to the *cis*-

vicinal diols and the configuration in methyl glycosides influenced the reactivity, but the selectivity of products was not changed. Moreover, the adsorption state and the tradition state were estimated by DFT calculations with structure isomers of methyl α-L-rhamnopyranoside and methyl α-L-fucopyranoside, which exhibit large reactivity difference (~5-fold). The difference of the reactivity is derived from that of the activation energy (65 kJ mol^{-1} and 77 kJ mol^{-1} for methyl α-L-rhamnopyranoside and methyl α-L-fucopyranoside), which was also supported by the kinetic results from Arrhenius plots (63 kJ mol^{-1} and 73 kJ mol^{-1} for methyl α-L-rhamnopyranoside and methyl α-L-fucopyranoside). We conclude that the reactivity difference of the methyl glycosides is mainly derived from that of the torsional angles, which is due to the intricate interaction between the OH group adjacent to the *cis*-vicinal OH groups and surface OH groups on CeO_2.

ASSOCIATED CONTENT

Supporting Information

This material is available free of charge via the Internet at http://pubs.acs.org.

Reagent information and experimental details; activity test results for the screening of catalysts and solvents; time-courses; raw kinetic data; the structures for DFT calculation.

AUTHOR INFORMATION

Corresponding Author

*mtamura@osaka-cu.ac.jp
*tomi@erec.che.tohoku.ac.jp

Notes

The authors declare no competing financial interest.

ACKNOWLEDGMENT

This work was supported by Grand–in–aid for Challenging Exploratory (18K18965), and partially supported by Grant–in–Aid for Scientific Research (S) (18H05247) from JSPS and Cooperative Research Program of Institute for Catalysis, Hokkaido University (Proposal 19A1006). Ji Cao thanks the China Scholarship Council for the financial support. Part of the calculations was performed on supercomputers at RCCS (Okazaki), RIIT (Kyushu Univ.), and the Center for Computational Materials Science, Institute for Materials Research (Tohoku University, Proposal No. 19S0006).

REFERENCES

(1) (a) Danishefsky, S. J.; Bilodeau, M. T., Glycals in Organic Synthesis: The Evolution of Comprehensive Strategies for the Assembly of Oligosaccharides and Glycoconjugates of Biological Consequence. *Angew. Chem. Int. Ed.* **1996**, *35*, 1380-1419. (b) Harris, J. M.; Keranen, M. D.; O'Doherty, G. A., Syntheses of D-and L-Mannose, Gulose, and Talose via Diastereoselective and Enantioselective Dihydroxylation Reactions. *J. Org. Chem.* **1999**, *64*, 2982-2983. (c) Allen, J. R.; Harris, C. R.; Danishefsky, S. J., Pursuit of Optimal Carbohydrate-Based Anticancer Vaccines: Preparation of A Multiantigenic Unimolecular Glycopeptide Containing the Tn, MBr1, and Lewis^y Antigens. *J. Am. Chem. Soc.* **2001**, *123*, 1890-1897. (d) Montero, A.; Mann, E.; Herradón, B., Preparation of Sugar Amino Acids by Claisen-Johnson Rearrangement: Synthesis and Incorporation into Enkephalin Analogues. *Eur. J. Org. Chem.* **2004**, *2004*, 3063-3073. (e) Boysen, M. M., Carbohydrates as Synthetic Tools in Organic Chemistry. *Chem. Eur. J.* **2007**, *13*, 8648-8659. (f) Henderson, A. S.; Bower, J. F.; Galan, M. C., Carbohydrates as Enantioinduction Components in Stereoselective Catalysis. *Org Biomol Chem* **2016**, *14*, 4008-4017. (g) Nahain, A. A.; Ignjatovic, V.; Monagle, P.; Tsanaktsidis, J.; Ferro, V., Heparin Mimetics with Anticoagulant Activity. *Med. Res. Rev.* **2018**, *38*, 1582-1613.

(2) (a) Stephanopoulos, G., Challenges in Engineering Microbes for Biofuels Production. *Science* **2007**, *315*, 801-804. (b) Haveren, J. v.; Scott, E. L.; Sanders, J., Bulk Chemicals from Biomass. *Biofuels, Bioprod. Biorefin.* **2008**, *2*, 41-57. (c) Dhepe, P. L.; Fukuoka, A. Cellulose Conversion under Heterogeneous Catalysis. *ChemSusChem* **2008**, *1*, 969-975. (d) Saxena, R. C.; Adhikari, D. K.; Goyal, H. B., Biomass-Based Energy Fuel through Biochemical Routes: A review. *Renew. Sust. Energ. Rev.* **2009**, *13*, 167-178. (e) Kobayashi, H.; Komanoya, T.; Guha, S. K.; Hara, K.; Fukuoka, A., Conversion of cellulose into renewable chemicals by supported metal catalysis. *Appl. Catal. A* **2011**, *409*, 13-20. (f) Melero, J. A.; Iglesias, J.; Garcia, A., Biomass as Renewable Feedstock in Standard Refinery Units. Feasibility, Opportunities and Challenges. *Energ. Environ. Sci.* **2012**, *5*, 7393-7420. (g) Kobayashi, H.; Fukuoka, A., Synthesis and utilisation of sugar compounds derived from lignocellulosic biomass. *Green Chem.* **2013**, *15*, 1740-1763. (h) Yang, Z. Q.; Wu, Y. Q.; Zhang, Z. S.; Li, H.; Li, X. G.; Egorov, R. I.; Strizhak, P. A.; Gao, X., Recent Advances in Co-Thermochemical Conversions of Biomass with Fossil Fuels Focusing On the Synergistic Effects. *Renew. Sust. Energ. Rev.* **2019**, *103*, 384-398. (i) Tursi, A., A Review on Biomass: Importance, Chemistry, Classification, and Conversion. *Biofuel Res. J.* **2019**, *6*, 962-979. (j) Leonard, M. D.; Michaelides, E. E.; Michaelides, D. N., Energy Storage Needs for the Substitution of Fossil Fuel Power Plants with Renewables. *Renew. Energ.* **2020**, *145*, 951-962.

(3) (a) Moreau, C.; Belgacem, M. N.; Gandini, A., Recent Catalytic Advances in the Chemistry of Substituted Furans from Carbohydrates and in the Ensuing Polymers. *Top. Catal.* **2004**, *27*, 11-30. (b) Huber, G. W.; Iborra, S.; Corma, A., Synthesis of Transportation Fuels from Biomass: Chemistry, Catalysts, and Engineering. *Chem. Rev.* **2006**, *106*, 4044-98. (c) Tanksale, A.; Wong, Y.; Beltramini, J.; Lu, G., Hydrogen Generation from Liquid Phase Catalytic Reforming of Sugar Solutions using Metal-Supported Catalysts. *Int. J. Hydrogen Energ.* **2007**, *32*, 717-724. (d) Binder, J. B.; Raines, R. T., Simple Chemical Transformation of Lignocellulosic Biomass into Furans for Fuels and Chemicals. *J. Am. Chem. Soc.* **2009**, *131*, 1979-85. (e) Ruppert, A. M.; Weinberg, K.; Palkovits, R., Hydrogenolysis Goes Bio: from Carbohydrates and Sugar Alcohols to Platform Chemicals. *Angew. Chem. Int. Ed.* **2012**, *51*, 2564-601. (f) Bender, T. A.; Dabrowski, J. A.; Gagne, M. R., Homogeneous catalysis for the production of low-volume, high-value chemicals from biomass. *Nat. Rev. Chem.* **2018**, *2*, 35-46. (g) Yang, W.; Du, X.; Liu, W.; Wang, Z.; Dai, H.; Deng, Y., Direct Valorization of Lignocellulosic Biomass into Value-Added Chemicals by Polyoxometalate Catalyzed Oxidation under Mild Conditions. *Ind. Eng. Chem. Res.* **2019**, *58*, 22996-23004.

(4) Tamura, M.; Nakagawa, Y.; Tomishige, K., Reduction of sugar derivatives to value chemicals ~utilization of asymmetric carbons~. *Catal. Sci. Technol.* **2020**, 10, 3805-3824.

(5) Muramatsu, W.; Tanigawa, S.; Takemoto, Y.; Yoshimatsu, H.; Onomura, O., Organotin-Catalyzed Highly Regioselective Thiocarbonylation of Nonprotected Carbohydrates and Synthesis of Deoxy Carbohydrates in A Minimum Number of Steps. *Chem. Eur. J.* **2012**, *18*, 4850-4853.

(6) Adduci, L. L.; Bender, T. A.; Dabrowski, J. A.; Gagne, M. R., Chemoselective conversion of biologically sourced polyols into chiral synthons. *Nat. Chem.* **2015**, *7*, 576-581.

(7) (a) Bender, T. A.; Dabrowski, J. A.; Gagne, M. R., Delineating The Multiple Roles of $B(C_6F_5)_3$ in the Chemoselective Deoxygenation of Unsaturated Polyols. *ACS Catal.* **2016**, *6*, 8399-8403. (b) Bender, T. A.; Dabrowski, J. A.; Zhong, H.; Gagne, M. R., Diastereoselective $B(C_6F_5)_3$-Catalyzed Reductive Carbocyclization of Unsaturated Carbohydrates. *Org. Lett.* **2016**, *18*, 4120-3. (c) Lowe, J. M.; Seo, Y.; Gagne, M. R., Boron-Catalyzed Site-Selective

Reduction of Carbohydrate Derivatives with Catecholborane. *ACS Catal.* **2018**, *8*, 8192-8198.

(8) Cao, F.; Schwartz, T. J.; McClelland, D. J.; Krishna, S. H.; Dumesic, J. A.; Huber, G. W., Dehydration of cellulose to levoglucosenone using polar aprotic solvents. *Energ. Environ. Sci.* **2015**, *8*, 1808-1815.

(9) (a) Karanjkar, P. U.; Burt, S. P.; Chen, X. L.; Barnett, K. J.; Ball, M. R.; Kumbhalkar, M. D.; Wang, X. H.; Miller, J. B.; Hermans, I.; Dumesic, J. A.; Huber, G. W., Effect of carbon supports on RhRe bifunctional catalysts for selective hydrogenolysis of tetrahydropyran-2-methanol. *Catal. Sci. Technol.* **2016**, *6*, 7841-7851. (b) Krishna, S. H.; McClelland, D. J.; Rashke, Q. A.; Dumesic, J. A.; Huber, G. W., Hydrogenation of levoglucosenone to renewable chemicals. *Green Chem.* **2017**, *19*, 1278-1285.

(10) Larson, R. T.; Samant, A.; Chen, J.; Lee, W.; Bohn, M. A.; Ohlmann, D. M.; Zuend, S. J.; Toste, F. D., Hydrogen Gas-Mediated Deoxydehydration/Hydrogenation of Sugar Acids: Catalytic Conversion of Glucarates to Adipates. *J. Am. Chem. Soc.* **2017**, *139*, 14001-14004.

(11) (a) Dethlefsen, J. R.; Fristrup, P., Rhenium-Catalyzed Deoxydehydration of Diols and Polyols. *ChemSusChem* **2015**, *8*, 767-75. (b) Petersen, A. R.; Fristrup, P., New Motifs in Deoxydehydration: Beyond the Realms of Rhenium. *Chem. Eur. J.* **2017**, *23*, 10235-10243. (c) Wozniak, B.; Li, Y. H.; Tin, S.; de Vries, J. G., Rhenium-Catalyzed Deoxydehydration of Renewable Triols Derived from Sugars. *Green Chem.* **2018**, *20*, 4433-4437. (d) DeNike, K. A.; Kilyanek, S. M., Deoxydehydration of Vicinal Diols by Homogeneous Catalysts: A Mechanistic Overview. *R. Soc. Open Sci.* **2019**, *6*, 191165. (e) Donnelly, L. J.; Thomas, S. P.; Love, J. B., Recent Advances in the Deoxydehydration of Vicinal Diols and Polyols. *Chem. Asian J.* **2019**, *14*, 3782-3790. (f) Tshibalonza, N. N.; Monbaliu, J.-C. M., The deoxydehydration (DODH) reaction: a versatile technology for accessing olefins from bio-based polyols. *Green Chem.* **2020**, 22, 4801-4848.

(12) (a) Arceo, E.; Ellman, J. A.; Bergman, R. G., Rhenium-Catalyzed Didehydroxylation of Vicinal Diols to Alkenes using A Simple Alcohol as A Reducing Agent. *J. Am. Chem. Soc.* **2010**, *132*, 11408-11409. (b) Li, X.; Wu, D.; Lu, T.; Yi, G.; Su, H.; Zhang, Y., Highly Efficient Chemical Process to Convert Mucic Acid into Adipic Acid and DFT Studies of the Mechanism of the Rhenium-Catalyzed Deoxydehydration. *Angew. Chem. Int. Ed.* **2014**, *53*, 4200-4204. (c) Michael McClain, J.; Nicholas, K. M., Elemental Reductants for the Deoxydehydration of Glycols. *ACS Catal.* **2014**, *4*, 2109-2112. (d) Raju, S.; Moret, M.-E.; Klein Gebbink, R. J. M., Rhenium-Catalyzed Dehydration and Deoxydehydration of Alcohols and Polyols: Opportunities for the Formation of Olefins from Biomass. *ACS Catal.* **2014**, *5*, 281-300. (e) Larson, R. T.; Samant, A.; Chen, J.; Lee, W.; Bohn, M. A.; Ohlmann, D. M.; Zuend, S. J.; Toste, F. D., Hydrogen Gas-Mediated Deoxydehydration/Hydrogenation of Sugar Acids: Catalytic Conversion of Glucarates to Adipates. *J. Am. Chem. Soc.* **2017**, *139*, 14001-14004. (f) Shakeri, J.; Hadadzadeh, H.; Farrokhpour, H.; Weil, M., A Comparative Study of the Counterion Effect on the Perrhenate-Catalyzed Deoxydehydration Reaction. *Mol. Catal.* **2019**, *471*, 27-37. (g) Li, J.; Lutz, M.; Klein Gebbink, R. J. M., N,N,O-Coordinated tricarbonylrhenium precatalysts for the aerobic deoxydehydration of diols and polyols. *Catal. Sci. Technol.* **2020**, 10, 3782-3788.

(13) Murru, S.; Nicholas, K. M.; Srivastava, R. S. Ruthenium (II) sulfoxides-catalyzed hydrogenolysis of glycols and epoxides. *J. Mol. Catal. A: Chem.* **2012**, 363–364, 460–464.

(14) Dethlefsen, J. R.; Lupp, D.; Teshome, A.; Nielsen, L. B.; Fristrup, P., Molybdenum-Catalyzed Conversion of Diols and Biomass-Derived Polyols to Alkenes Using Isopropyl Alcohol as Reductant and Solvent. *ACS Catal.* **2015**, *5*, 3638-3647.

(15) Petersen, A. R.; Nielsen, L. B.; Dethlefsen, J. R.; Fristrup, P., Vanadium-Catalyzed Deoxydehydration of Glycerol Without an External Reductant. *ChemCatChem* **2018**, *10*, 769-778.

(16) (a) Denning, A. L.; Dang, H.; Liu, Z.; Nicholas, K. M.; Jentoft, F. C., Deoxydehydration of Glycols Catalyzed by Carbon-Supported Perrhenate. *ChemCatChem* **2013**, *5*, 3567-3570. (b) Sun, R.; Zheng, M.; Li, X.; Pang, J.; Wang, A.; Wang, X.; Zhang, T., Production of renewable 1,3-pentadiene from xylitol via formic acid-mediated deoxydehydration and palladium-catalyzed deoxygenation reactions. *Green Chem.* **2017**, *19*, 638-642. (c) Lin, J.; Song, H.; Shen, X.; Wang, B.; Xie, S.; Deng, W.; Wu, D.; Zhang, Q.; Wang, Y., Zirconia-supported rhenium oxide as an efficient catalyst for the synthesis of biomass-based adipic acid ester. *Chem Commun* **2019**, *55*, 11017-11020. (d) MacQueen, B.; Barrow, E.; Rivera Castro, G.; Pagan-Torres, Y.; Heyden, A.; Lauterbach, J., Optimum Reaction Conditions for 1,4-Anhydroerythritol and Xylitol Hydrodeoxygenation over a ReO_x–Pd/CeO_2 Catalyst via Design of Experiments. *Ind. Eng. Chem. Res.* **2019**, 58, 8681-8689. (e) MacQueen, B.; Ruiz-Yi, B.; Royko, M.; Heyden, A.; Pagan-Torres, Y. J.; Williams, C.; Lauterbach, J., In-Situ Oxygen Isotopic Exchange Vibrational Spectroscopy of Rhenium Oxide Surface Structures on Cerium Oxide. *J. Phys. Chem. C* **2020**, 124, 7174-7181.

(17) (a) Sandbrink, L.; Beckerle, K.; Meiners, I.; Liffmann, R.; Rahimi, K.; Okuda, J.; Palkovits, R., Supported Molybdenum Catalysts for the Deoxydehydration of 1,4-Anhydroerythritol into 2,5-Dihydrofuran. *ChemSusChem* **2017**, *10*, 1375-1379. (b) Xi, Y.; Lauterbach, J.; Pagan-Torres, Y.; Heyden, A., Deoxydehydration of 1,4-Anhydroerythritol over Anatase TiO_2(101)-Supported ReO_x and MoO_x. *Catal. Sci. Technol.* **2020**, 10, 3731-3738.

(18) Nijem, S.; Dery, S.; Carmiel, M.; Horesh, G.; Garrevoet, J.; Spiers, K.; Falkenberg, G.; Marini, C.; Gross, E., Bimetallic Pt–Re Nanoporous Networks: Synthesis, Characterization, and Catalytic Reactivity. *J. Phys. Chem. C* **2018**, *122*, 24801-24808.

(19) Jang, J. H.; Sohn, H.; Camacho-Bunquin, J.; Yang, D. L.; Park, C. Y.; Delferro, M.; Abu-Omar, M. M., Deoxydehydration of Biomass-Derived Polyols with a Reusable Unsupported Rhenium Nanoparticles Catalyst. *ACS Sustain. Chem. Eng.* **2019**, *7*, 11438-11447.

(20) Tamura, M.; Yuasa, N.; Cao, J.; Nakagawa, Y.; Tomishige, K., Transformation of Sugars into Chiral Polyols over a Heterogeneous Catalyst. *Angew. Chem. Int. Ed.* **2018**, *57*, 8058-8062.

(21) Cao, J.; Tamura, M.; Nakagawa, Y.; Tomishige, K., Direct Synthesis of Unsaturated Sugars from Methyl Glycosides. *ACS Catal.* **2019**, *9*, 3725-3729.

(22) (a) Ota, N.; Tamura, M.; Nakagawa, Y.; Okumura, K.; Tomishige, K., Hydrodeoxygenation of Vicinal OH Groups over Heterogeneous Rhenium Catalyst Promoted by Palladium and Ceria Support. *Angew. Chem. Int. Ed.* **2015**, *54*, 1897-1900. (b) Ota, N.; Tamura, M.; Nakagawa, Y.; Okumura, K.; Tomishige, K., Performance, Structure, and Mechanism of ReO_x–Pd/CeO_2 Catalyst for Simultaneous Removal of Vicinal OH Groups with H_2. *ACS Catal.* **2016**, *6*, 3213-3226.

(23) (a) Tazawa, S.; Ota, N.; Tamura, M.; Nakagawa, Y.; Okumura, K.; Tomishige, K., Deoxydehydration with Molecular Hydrogen over Ceria-Supported Rhenium Catalyst with Gold Promoter. *ACS Catal.* **2016**, *6*, 6393-6397. (b) Nakagawa, Y.; Tazawa, S.; Wang, T.; Tamura, M.; Hiyoshi, N.; Okumura, K.; Tomishige, K., Mechanistic Study of Hydrogen-Driven Deoxydehydration over Ceria-Supported Rhenium Catalyst Promoted by Au Nanoparticles. *ACS Catal.* **2017**, *8*, 584-595.

(24) (a) Danishefsky, S. J.; Armistead, D. M.; Wincott, F. E.; Selnick, H. G.; Hungate, R. The Total Synthesis of Avermectin A1a. *J. Am. Chem. Soc.* **1989**, 111, 2967–2980. (b)Danishefsky, S. J.; Bilodeau, M. T. Glycals in Organic Synthesis: The Evolution of Comprehensive Strategies for the Assembly of Oligosaccharides and Glycoconjugates of Biological Consequence. *Angew. Chem., Int. Ed.* **1996**, 35, 1380–1419. (c) Křen, V.; Řezanka,T., Sweet antibiotics – the role of glycosidic residues in antibiotic and antitumor activity and their randomization. *FEMS Microbiol. Rev.* **2008**, 32,858–859.

(25) Krishna, S. H.; Cao, J.; Tamura, M.; Nakagawa, Y.; De Bruyn, M.; Jacobson, G. S.; Weckhuysen, B. M.; Dumesic, J. A.; Tomishige, K.; Huber, G. W., Synthesis of Hexane-Tetrols and -Triols with Fixed Hydroxyl Group Positions and Stereochemistry from Methyl

Glycosides over Supported Metal Catalysts. *ACS Sustain. Chem. Eng.* **2020**, *8*, 800-805.

(26) Corma, A.; Iborra, S.; Velty, A., Chemical Routes for the Transformation of Biomass into Chemicals. *Chem. Rev*. **2007**, 107, 2411–2502.

(27) Krishna, S. H.; Schmidt, Z. R.; Weckhuysen, B. M.; Dumesic, J. A.; Huber, G. W., Catalytic Production of Hexane-1, 2, 5, 6-Tetrol from Bio-Renewable Levoglucosanol in Water: Effect of Metal and Acid Sites on (Stereo)-Selectivity. *Green Chem.* **2018**, *20*, 4557-4565.

(28) Tamagawa, K.; Hilderbrandt, R. L.; Shen, Q., Molecular-Structure of Cyclopentanone by Gas-Phase Electron-Diffraction. *J. Am. Chem. Soc.* **1987**, *109*, 1380-1383.

(29) (a) Chen, K.; Mori, K.; Watanabe, H.; Nakagawa, Y.; Tomishige, K., C–O Bond Hydrogenolysis of Cyclic Ethers with OH Groups over Rhenium-Modified Supported Iridium Catalysts. *J. Catal.* **2012**, *294*, 171-183. (b) Amada, Y.; Watanabe, H.; Hirai, Y.; Kajikawa, Y.; Nakagawa, Y.; Tomishige, K., Production of Biobutanediols by The Hydrogenolysis of Erythritol. *ChemSusChem* **2012**, *5*, 1991-1999.

(30) Xi, Y. J.; Yang, W. Q.; Ammal, S. C.; Lauterbach, J.; Pagan-Torres, Y.; Heyden, A., Mechanistic Study of the Ceria Supported, Re-Catalyzed Deoxydehydration of Vicinal OH Groups. *Catal. Sci. Technol.* **2018**, *8*, 5740-5752.

(31) Liu, P.; Nicholas, K. M., Mechanism of Sulfite-Driven, $MeReO_3$-Catalyzed Deoxydehydration of Glycols. *Organometallics* **2013**, *32*, 1821-1831.

.

SYNOPSIS TOC